Superconductivity in repulsively interacting fermions on a diamond chain: Flat-band-induced pairing

Keita Kobayashi,[1] Masahiko Okumura,[1] Susumu Yamada,[1,2] Masahiko Machida,[1] and Hideo Aoki[3,4]
[1]*CCSE, Japan Atomic Energy Agency, Kashiwa, Chiba 277-0871, Japan*
[2]*Computational Materials Science Research Team, RIKEN AICS, Kobe, Hyogo 650-0047, Japan*
[3]*Department of Physics, University of Tokyo, Hongo, Tokyo 113-0033, Japan*
[4]*Electronics and Photonics Research Institute, Advanced Industrial Science and Technology (AIST), Tsukuba, Ibaraki 305-8568, Japan*
(Received 12 August 2016; revised manuscript received 23 October 2016; published 1 December 2016)

To explore whether a flat-band system can accommodate superconductivity, we consider repulsively interacting fermions on the diamond chain, a simplest possible quasi-one-dimensional system that contains a flat band. Exact diagonalization and the density-matrix renormalization group are used to show that we have a significant binding energy of a Cooper pair with a long-tailed pair-pair correlation in real space when the total band filling is slightly below 1/3, where a filled dispersive band interacts with the flat band that is empty but close to E_F. Pairs selectively formed across the outer sites of the diamond chain are responsible for the pairing correlation. At exactly 1/3-filling an insulating phase emerges, where the entanglement spectrum indicates the particles on the outer sites are highly entangled and topological. These come from a peculiarity of the flat band in which "Wannier orbits" are not orthogonalizable.

DOI: 10.1103/PhysRevB.94.214501

I. INTRODUCTION

While the fascination with unconventional superconductivity arising from electron correlation continues to increase, as exemplified by the high-T_C cuprates and iron-based superconductors, a next question to ask is whether there exists an avenue where we have superconductivity with another pairing mechanism. Namely, in the superconductivity in correlated electron systems, the standard viewpoint is that the interaction mediated by spin fluctuations glues the electrons into anisotropic pairs such as d wave or s_{+-}, where the nesting of the Fermi surface dominates the fluctuation, hence the superconductivity. To look for a different class of models, one intriguing direction is to consider correlated systems on flat-band lattices that contain dispersionless band(s) in their band structure. This is because, regardless of the Fermi energy residing on or off the flat band, we cannot define the Fermi surface for the flat band. In other words, we cannot apply, in one-dimensional cases, the Tomonaga-Luttinger picture for the states around E_F even with multichannel g-ology unlike the case of ladders. Thus, if superconductivity does arise, this might harbor a mechanism in which the flat band plays a role distinct from the conventional, nesting-dominated boson-exchange mechanisms.

In the field of ferromagnetism, on the other hand, there is a long history of the study of flat-band ferromagnetism [1–3], which is distinct from the conventional (Stoner) ferromagnetism. The ferromagnetic ground state is rigorously shown for arbitrary repulsive interaction $0 < U \leqslant \infty$ when the flat band is half-filled. The flat-band lattice models are conceived as a Lieb model [1] with different numbers of A and B sublattice sites, or as Mielke and Tasaki models [2,3] such as kagome lattice. A speciality of these flat-band lattices appears as an anomalous situation that Wannier orbitals cannot be orthogonalized, which is called the connectivity condition for the density matrix [4]. This immediately dictates that the flat band arises from interferences, hence totally different from the atomic (zero-hopping) limit, and indeed the flat-band models are necessarily multiband systems, where the flat band(s) coexist with dispersive ones. Flat-band systems are not merely a theoretical curiosity, but candidate systems have been considered [5]. Also, recent developments in cold-atom Fermi gases on optical lattices are a promising arena, where Lieb [6] and kagome [7] lattices are already realized.

Thus the flat-band system provides a unique playground, because the correlation effects should be strong for the flat bands (as briefly described in Appendix C), but also because of the above-mentioned unusual structure of the density matrix (or strongly interfering wave functions). We can thus envisage dramatic, possibly nonperturbative phenomena from the electron-electron interaction on these macroscopically degenerate manifolds of single-particle states. Besides the ferromagnetism, the flat-band systems have attracted recent attention for possible realization of topological insulators with nontrivial Chern numbers [8–12]. The next goal, in our view, is to realize superconductivity in flat-band systems. We shall show here that there are indeed signatures for pairing for repulsive interaction electrons in a one-dimensional flat-band lattice.

Theoretically, exploration of superconducting phases in flat-band systems is quite challenging, since correlation effects become even more difficult to fathom for the flat bands than in ordinary ones [13]. Thus far, the possibility of pair formation on flat bands has been examined by several authors. The pairing of two fermions on a diamond chain with π flux inserted was discussed by Vidal *et al.* [14]. Kuroki *et al.* have considered a cross-linked ladder that contains wide and narrow (or flat) bands in the context of the high-T_C cuprate ladder compound [15], and have shown that superconducting T_C estimated from the fluctuation exchange approximation (FLEX) is much higher than in usual lattices when E_F is just above the flat band that pierces the dispersive one. There, virtual pair scatterings between the dispersive and fully filled flat bands are suggested to cause the high T_C. Pair formation has also been discussed for the Bose-Hubbard model on cross-linked ladders [16,17], where a large pair hopping gives rise to the emergence of a

 ©2016 American Physical Society

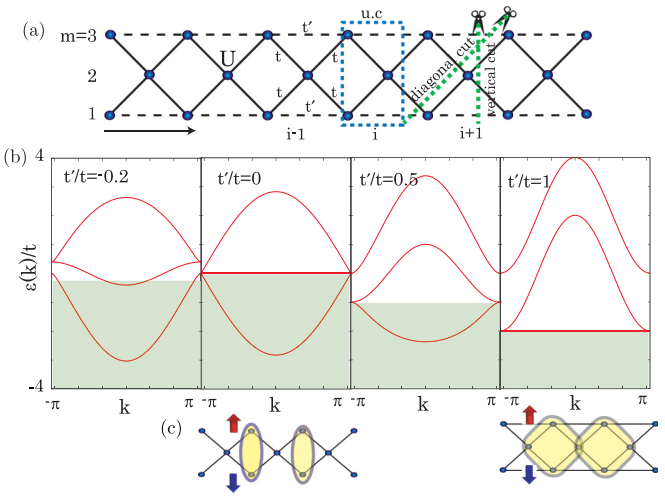

FIG. 1. (a) Hubbard model on a diamond chain with t (t') the nearest-neighbor (interapex) hoppings, m labeling the leg, while i is the unit cell. Also shown are two types of cuts (vertical and diagonal), which are used in DMRG calculation of the entanglement entropy. (b) Band structures in the noninteracting case ($U = 0$) for various values of t', with shaded areas indicating the 1/3-filling. (c) Orbits considered here for the flat band at $t'/t = 0$ or 1.

superfluid phase (pair Tomonaga-Luttinger liquid) overlapping with a Wigner-solid region in the phase diagram. Namely, in flat-band systems, not only pair hopping amplitudes can be large, but also diagonal orders tend to coexist (rather than compete) with superfluids. These results suggest that the flat bands may indeed be a good place to look for pair condensates.

This has motivated us here to explore superconductivity for a repulsive fermionic Hubbard model on flat-band systems. As a model we take a simplest possible, quasi-one-dimensional (quasi-1D) lattice comprising a chain of diamonds as depicted in Fig. 1(a). We shall show that for E_F close to but slightly below the flat band (with the filling of the whole bands slightly below 1/3), attractive binding energies appear. Concomitantly, the pair-pair correlation becomes long tailed in real space at these band fillings.

II. MODEL AND METHODS

As methods for calculation we opt for exact diagonalization and the density-matrix renormalization group (DMRG) that can deal with strong correlation, since the correlation phenomena on flat bands may well call for such nonperturbative methods. For the position of the Fermi energy, E_F, we focus on the regime where the flat band is empty. This choice comes from the following observation. When the flat band is half filled, the ground state is ferromagnetic. When E_F is shifted but still on the flat band, the diverging density of one-electron states is expected to give rise to large self-energy corrections, which should be detrimental to superconductivity. When the flat band is empty with E_F residing in a dispersive band, this problem can be resolved, with virtual processes between the dispersive and flat bands still at work. For bipartite lattices such as the diamond chain, the empty flat band is equivalent to a fully filled flat band due to an electron-hole symmetry.

It is desirable to have, on top of E_F, another control parameter about the flat band. So here we introduce a hopping t' between the adjacent apex sites of diamonds [Fig. 1(a)]. For $t' = 0$ the lattice (a Lieb model) is bipartite with the flat band as a middle one in this three-band system. As we increase t' the bands are deformed, until in the limit $t'/t = 1$ the bottom band becomes flat (a Mielke model). Thus we can examine how the pairing behaves as we change $t' = 0 \to 1$. We then calculate the binding energy of pairs with the exact diagonalization (ED), and pair-pair (and other) correlation functions with the DMRG [18–21].

We take the conventional Hubbard Hamiltonian on the diamond chain [Fig. 1(a)],

$$H = H_{\rm kin} + H_{\rm int}, \tag{1}$$

$$H_{\rm kin} = t \sum_{i,\sigma=\uparrow\downarrow} c^{\dagger}_{2,i,\sigma} \sum_{m=1,3} (c_{m,i,\sigma} + c_{m,i+1,\sigma}) + t' \sum_{i,\sigma=\uparrow\downarrow} \sum_{m=1,3} c^{\dagger}_{m,i,\sigma} c_{m,i+1,\sigma} + \text{H.c.}, \tag{2}$$

$$H_{\rm int} = U \sum_{m,i} n_{m,i,\uparrow} n_{m,i,\downarrow}, \tag{3}$$

where t (unit of energy) and t' are the nearest-neighbor and interapex hoppings, respectively, $c^{\dagger}_{m,i,\sigma}$ creates a fermion with spin σ on the mth leg at the ith unit cell, $n_{m,i,\sigma} = c^{\dagger}_{m,i,\sigma} c_{m,i,\sigma}$, and $U > 0$ is the on-site repulsive interaction. Figure 1(b) shows the band structure, $\epsilon(k) = \pm\{4[1 + \cos(k)] + (t')^2 \cos^2(k)\}^{1/2} + t' \cos(k)$, $2t' \cos(k)$, in the noninteracting case ($U = 0$). As we can see, one of the three bands becomes flat in the limit of $t' = 0$ or 1. We focus on the region where the filling of the whole bands is around 1/3 (one fermion per unit cell on average) to investigate the effects of repulsive interaction. We have, for $t' = 0 \to 1$, a fully occupied bottom band which touches the middle band at $k = \pm\pi$, where the middle (bottom) band becomes flat at $t' = 0$ (1).

Intriguingly, we have noticed in performing the DMRG that we have to keep an unusually large number of states up to $m_{\rm DMRG} = 1500$ for the present ladderlike lattice. For DMRG we take an open boundary condition with inversion-symmetric configurations as shown in Fig. 1(a). Here we focus on the properties below 1/3-filling to explore the possibility of fermion superfluidity in terms of the pair binding energy and correlation functions.

III. RESULTS

Let us first examine the fermion pair formation in terms of the binding energy, $\Delta E_b \equiv E_g(N_\uparrow + 1, N_\downarrow + 1) + E_g(N_\uparrow, N_\downarrow) - 2E_g(N_\uparrow + 1, N_\downarrow)$, where $E_g(N_\uparrow, N_\downarrow)$ is the ground-state energy for $N_{\rm tot} = N_\uparrow + N_\downarrow$ fermions with N_σ being the total number of σ-spin electrons. A negative ΔE_b implies that an attractive interaction works between two particles. $E_g(N_\uparrow, N_\downarrow)$ is computed with ED in periodic boundary conditions. In the numerical calculation, we set the total number of sites to be $N = 18$ with the length of the chain being $L = N/3 = 6$.

Figure 2(a) shows ΔE_b as a function of the filling $n = N_{\rm tot}/2N$ for $t' = 0$ for various values of U/t. We can

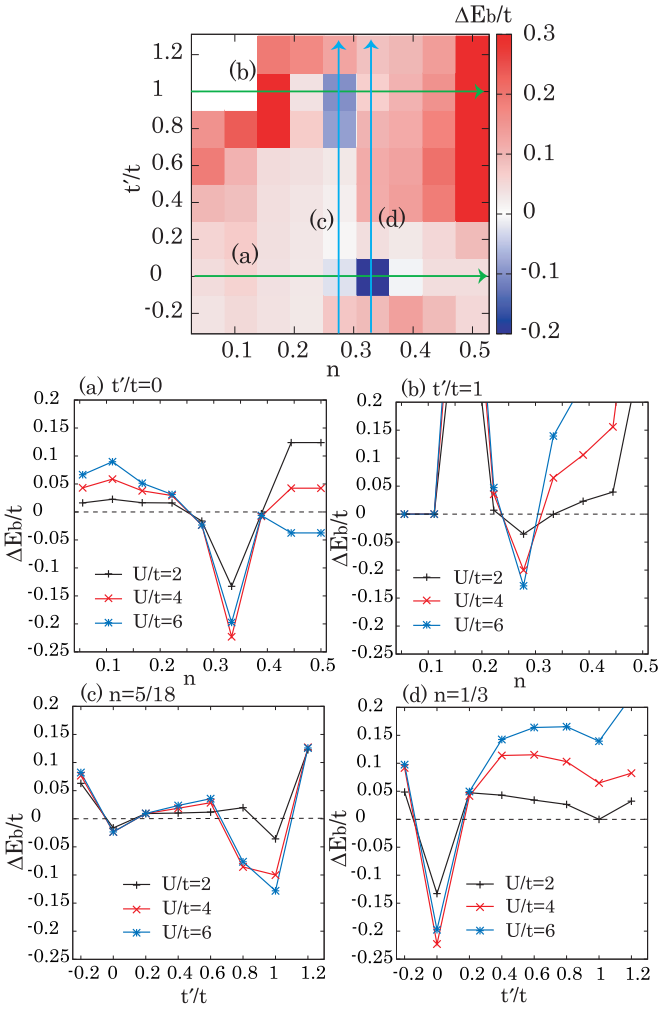

FIG. 2. (a), (b) ED result for the binding energy ΔE_b vs band filling n for $t' = 0$ (a) or $t'/t = 1$ (b) for various values of U/t with $N = 18$ sites here. (c), (d) Binding energy ΔE_b vs t'/t for band filling $n = 5/18$ (c) or $n = 1/3$ (d) for various values of U/t. Top panel is a color-code plot of ΔE_b against n and t'/t for $U/t = 4$, where arrows indicate the cross sections displayed in panels (a)–(d).

immediately notice that two electrons become bound (i.e., ΔE_b becomes negative) sharply around $n = 1/3$ ($N_\uparrow = N_\downarrow = 6$, $N = 18$) for all the values of $U > 0$ considered. Interestingly, the binding energy is not monotonic against U but peaked around $U/t = 4$. As we shall see, the binding occurs for two electrons sitting on the $m = 1$ and 3 legs. The binding energy continues to be negative just below $n = 1/3$. In the other flat-band limit at $t'/t = 1$, we can see in Fig. 2(b) that we have again a binding at a filling slightly smaller than 1/3 (5/18-filling), where ΔE_b becomes negative, but this causes a phase separation between insulator and CDW-like phase in the case of $t'/t = 1$ as shown in Appendix B.

We now proceed to DMRG calculations for various correlation functions, including pair correlation for $t' = 0$ [22]. The density (D_m) and spin (S_m) correlation functions on the mth leg are defined, respectively, as

$$D_m(i,j) = \langle n_{m,i} n_{m,j} \rangle - \langle n_{m,i} \rangle \langle n_{m,i} \rangle, \tag{4}$$

$$S_m(i,j) = \langle S^{(z)}_{m,i} S^{(z)}_{m,j} \rangle, \tag{5}$$

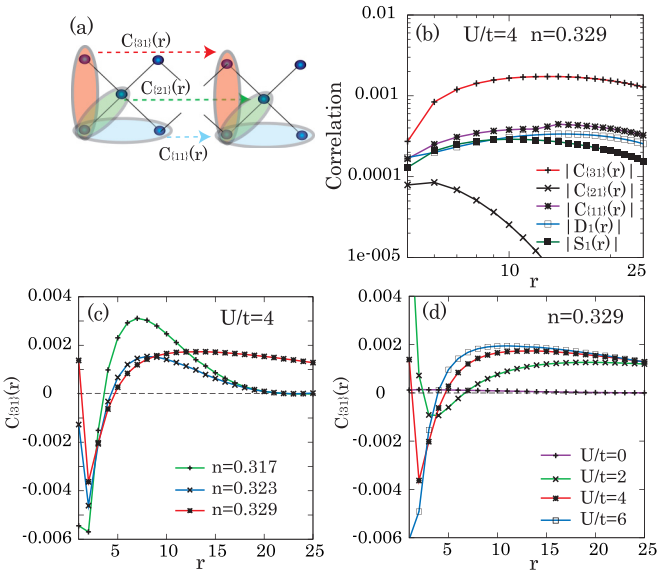

FIG. 3. (a) Correlation of various possible pair configurations on the diamond chain with $t' = 0$. (b) Absolute values of various pair correlation functions are shown against real-space distance r along with density and spin correlation functions for $U/t = 4$, $n = 0.329$. (c) Pair correlation $C^{\text{pair}}_{\{31\}}(r)$ against r for various values of n for $U/t = 4$. (d) Pair correlation $C^{\text{pair}}_{\{31\}}(r)$ for various values of U/t for $n = 0.329$. Here the length of the chain is $L = 55$ (with 164 sites in total).

with $n_{m,i} = n_{m,i,\uparrow} + n_{m,i,\downarrow}$ and $S^{(z)}_{m,i} = (n_{m,i,\uparrow} - n_{m,i,\downarrow})/2$. We compute the correlation functions on leg $m = 1$ and on 2 (while the correlation function on $m = 3$ is equivalent to those on $m = 1$). The singlet-pair correlation functions are defined as

$$C^{\text{pair}}_{\{m'm\}}(i,j) = \langle \Delta_{m'm,j} \Delta^\dagger_{m'm,i} \rangle, \tag{6}$$

$$\Delta_{m'm,i} \equiv c_{m',i+l,\uparrow} c_{m,i,\downarrow} - c_{m',i+l,\downarrow} c_{m,i,\uparrow}, \tag{7}$$

where l characterizes the pair [see Fig. 3(a)].

The result for various correlations in Fig. 3(b) reveals that the dominant (most long tailed with distance r) correlation for $U/t \neq 0$ in the vicinity of 1/3-filling ($n \simeq 0.329$ with $N_\uparrow = N_\uparrow = 54$ and $N = 164$) is the pair correlation $|C^{\text{pair}}_{\{31\}}(r)|$ for the pair,

$$\Delta_{31,i} = c_{3,i,\uparrow} c_{1,i,\downarrow} - c_{3,i,\downarrow} c_{1,i,\uparrow},$$

across $m = 1$ and 3 [see Fig. 3(a)] [24]. The next dominant correlations are the pair $C^{\text{pair}}_{\{11\}}(r)$ (for $\Delta_{11,i} = c_{1,i+1,\uparrow} c_{1,i,\downarrow} - c_{1,i+1,\downarrow} c_{1,i,\uparrow}$) and density $D_1(r)$ correlations on $m = 1$. Then comes the spin $S_1(r)$ correlation on $m = 1$. On the other hand, the correlations on $m = 2$ [see $C^{\text{pair}}_{\{21\}}(r)$ and Appendix B] rapidly decay for all the values of n studied here [22]. As in the density and spin correlations, the pair correlation involving $m = 2$ ($\Delta_{21,i} = c_{2,i,\uparrow} c_{1,i,\downarrow} - c_{2,i,\downarrow} c_{1,i,\uparrow}$) shows a fast decay. The dominant $\Delta_{31,i}$ is consistent with an analysis of the entanglement entropy and edge states at $t' = 0$ in Appendix A.

The reason why all of the pair, density, and spin correlations develop on legs $m = 1,3$ in the vicinity of 1/3-filling can be considered as coming from the basis functions on the flat band.

When the hopping t' is absent, we can introduce a basis,

$$\alpha_{i,\sigma} = c_{2,i,\sigma}, \qquad \beta_{i,\sigma} = (c_{1,i,\sigma} + c_{3,i,\sigma})/\sqrt{2},$$
$$\gamma_{i,\sigma} = (c_{1,i,\sigma} - c_{3,i,\sigma})/\sqrt{2}, \tag{8}$$

with which the kinetic part of Eq. (1) can be expressed as $H_{\mathrm{kin},t'=0} = \sqrt{2}t \sum_{i,\sigma} \alpha^{\dagger}_{i,\sigma}(\beta_{i,\sigma} + \beta_{i-1,\sigma}) + \mathrm{H.c.}$ The basis $\{\gamma_{i,\sigma}\}$ represents the particles on the flat band [see left panel of Fig. 1(c)], in which the probability amplitude selectively resides on legs $m = 1$ and 3 (i.e., on the A sublattice if we divide the bipartite lattice). The interaction U then brings about interband matrix elements between the flat and dispersive bands around 1/3-filling. The development of superconductivity when the flat band is empty (which is equivalent to full filling in the present electron-hole symmetric lattice) is consistent with the result in Ref. [15]. While the latter uses FLEX, a weak-coupling method, the present result reveals the flat-band superconductivity is in fact prominent in a strong-coupling ($U/t \simeq 4$) regime. The behavior of the correlation functions enhanced on $m = 1,3$ should come from the virtual states that have probability amplitudes residing on legs $m = 1$ and 3 with the long-range nature of the correlations involving connected orbits for the flat band.

What happens when the filling is exactly 1/3 is also interesting, so that we have studied the quantum phases at that filling in Appendix A. Topological states are shown to emerge, which is indicated from the entanglement spectrum for spins on the outer sites as well as from emerging edge states. This is considered to be another effect of the unusual Wannier states in the flat band, and the pairing states for the E_F close to but away from the flat band seem to sit adjacent to a topological phase at the point where the flat band just becomes empty.

IV. SUMMARY

We have investigated repulsively interacting fermions on the diamond chain, a simplest possible quasi-1D flat-band system, with ED and DMRG calculations. The numerical results have revealed that when the band filling is slightly below 1/3 with the flat band close to but away from E_F, the pair binding energy calculated with ED has two sharp peaks at two flat-band limits ($t' = 0$ or 1). Then the DMRG shows that, for $t' = 0$, the most dominant correlation is the singlet pair across the outer sites ($m = 1,3$) of the diamond. For $t'/t = 1$, by constrast, a phase separated behavior is observed as indicated in Appendix B. The flat band promoting superconductivity through virtual pair hoppings involving the band as conceived in FLEX [15] is shown to be prominent in a strong-coupling regime. It is an interesting future problem to see whether a mechanism beyond the boson exchange is at work here, which will require methods that take account of vertex corrections.

While we have concentrated on the quasi-1D diamond chain, enhanced pairing correlations with the major component residing on the flat-band wave functions are expected to be a general property of the flat-band systems satisfying the connectivity condition, such as the Lieb lattice. Extension of the present study to flat-band systems with fluxes inserted [14,16,25] is also an interesting future work. While the diamond-chain structure has been discussed for condensed-matter systems such as an insulating magnet azurite [26,27], cold atoms on optical lattices should be an ideal test bench for experimental realizations of flat-band lattices.

ACKNOWLEDGMENTS

H.A. was supported by JSPS KAKENHI Grant No. 26247057 and ImPACT Project No. 2015-PM12-05-01 from JST. S.Y. and M.M. were partially supported by JSPS KAKENHI Grants No. 15K00178. M.M. was partially supported by JSPS KAKENHI Grants No. 26400322, and No. 16H02450. The numerical work was in part performed on Fujitsu BX900 at JAEA.

APPENDIX A: INSULATING PHASES AND EDGE STATES AT 1/3-FILLING

We present the results for the diamond chain exactly at 1/3-filling by evoking entanglement entropy and spectrum analysis. Entanglement entropy is a useful tool for distinguishing critical from gapped phases [28,29]. If a finite block of length ℓ is considered on a chain of L sites, the reduced density matrix is defined as $\rho_L(\ell) = \mathrm{Tr}_{L-\ell}|\Psi\rangle\langle\Psi|$, and the corresponding entanglement entropy (von Neumann entropy) is given by

$$S_L(\ell) = -\mathrm{Tr}\rho_L(\ell)\ln\rho_L(\ell). \tag{A1}$$

As is well known [28,29], if the system has a gapless excitation spectrum, the entanglement entropy should grow logarithmically with the block size ℓ. On the other hand, when all the excitations are gapped, $S_L(\ell)$ should tend to a constant for large ℓ. Furthermore, the eigenvalues (entanglement spectrum, ES) of the equation for the reduced density matrix, $\rho_L \boldsymbol{u}_k = \lambda_k \boldsymbol{u}_k$, contain rich information on bulk properties. For instance, degeneracies of ES determine the parity of the many-body wave functions and distinguish nontrivial topological states from trivial product states [30,31]. In addition, doubly degenerate ES in the bulk indicates doubly degenerate edge spectrum in finite systems.

First, we focus on the original diamond chain with $t' = 0$ for filling $n = \frac{N_{\mathrm{tot}}}{2N} \simeq 0.337$, where N_{tot} (=70 here) is the total number of particles and N (=104) is the total number of sites. The filling 0.337 corresponds to 1/3-filling in the periodic boundary condition, where the bottom dispersive band is fully occupied and touches the flat band at $k = \pm\pi$ [see Fig. 1(b) in the main text]. In calculating the entanglement entropy, we can introduce two types of cuts of the diamond chain, namely vertical and diagonal cuts as shown in Fig. 1(a) in the main text. Insets of Figs. 4(a) and 4(b) show the entanglement entropy $S(\ell)$ against the block length ℓ for the vertical and diagonal cuts. We can see in both cases that the initial slope of $S_L(\ell)$ vs ℓ for $U/t = 0$ shows a logarithmic growth as a consequence of gapless excitations. As U/t is increased, $S_L(\ell)$ rapidly saturates to a constant, which implies a phase transition from gapless to gapped phases induced by repulsive U. Note that this phase transition is distinct from the Mott transition at half-filling: All the excitation spectra are gapped and transition occurs at 1/3-filling.

If we turn to eigenvalues of the reduced density matrix (entanglement spectrum), it is known that ES can depend on how the system is divided into subsystems [33,34]. Figures 4(a) and 4(b) respectively show the ES for the vertical

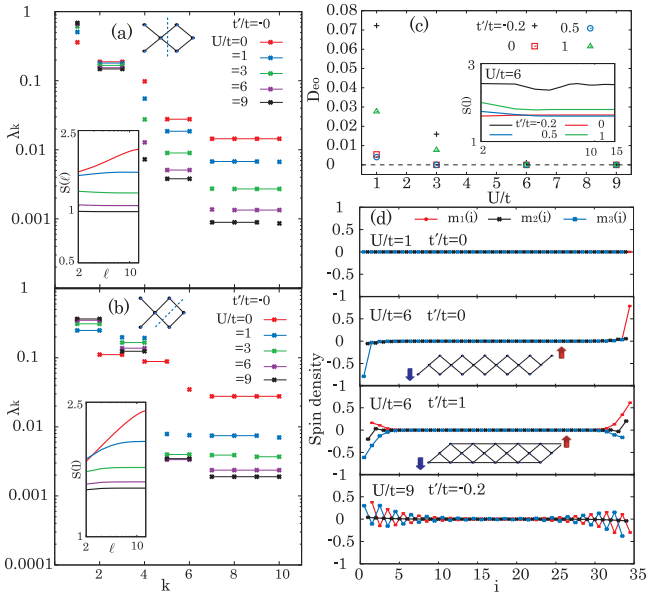

FIG. 4. Eigenvalues of the reduced density matrix λ_k versus the eigenvalue number k for vertical (a) or diagonal (b) cuts for various values of U/t with $t' = 0$. Degenerate values are connected by horizontal lines. Respective insets show the entanglement entropy $S(\ell)$ against the block length ℓ on double logarithmic scales for $t' = 0$. (c) $D_{\rm eo} = \sum_{k=1}^{N=100}(\lambda_{2k} - \lambda_{2k-1})/\lambda_{2k-1}$ (see text) against the interaction U/t for the diagonal cut for various values of t'. Inset shows the corresponding entanglement entropy $S(\ell)$ against ℓ for $U/t = 6$. (d) Spin density profiles on leg $m = 1$ (red), $m = 2$ (black), and $m = 3$ (blue) for, from top to bottom, $U/t = 1$, $t' = 0$; $U/t = 6$, $t' = 0$; $U/t = 6$, $t'/t = 1$, and $U/t = 9$, $t'/t = -0.2$ for diagonal cuts.

and diagonal cuts, where we incise the system at the center of the chain. We find that the ES for the vertical cut has no even degeneracies for all the values of the interaction studied here, whereas even degeneracies appear for the diagonal cut when the interaction U/t becomes large. ES behavior goes hand in hand with edge states, which is known as the bulk-edge correspondence. The spin density profile in Fig. 4(d) reveals that, while ES degeneracies are not developed for $U/t = 1$ [see the values at $k = 9,10$ in Fig. 4(a)], edge states (accommodating free 1/2 spins) do emerge around the diagonally-cut boundaries for a larger $U/t = 6$, where the even degeneracies are clearly seen. In this sense the diagonal cut here may be similar to cutting a spin singlet in the Haldane model [32].

Next, we turn to the case with $t' \neq 0$. Let us define a quantity $D_{\rm eo} = \sum_{k=1}^{N}(\lambda_{2k} - \lambda_{2k-1})/\lambda_{2k-1}$ as a measure of the even-odd degeneracy of ES: $D_{\rm eo}$ should vanish for even degeneracies. In Fig. 4(c), the even degeneracy for diagonal cut can be observed for all the values of t' for strong enough interaction U/t. As in the $t' = 0$ case, the degeneracy is seen to arise when the gapped phase is formed, where the entanglement entropy $S(\ell)$ becomes constant for large ℓ [see inset of Fig. 4(c)]. We note that even degeneracies for vertical cut do not emerge as in $t' = 0$. In lower panels in Fig. 4(d) the edge states derived from the even degeneracies are seen to exhibit various structures depending on the value of t': Edge states for $t' = 1$ broaden over several lattice sites and across different legs (m), in contrast to the $t' = 0$ case where edge states are highly localized

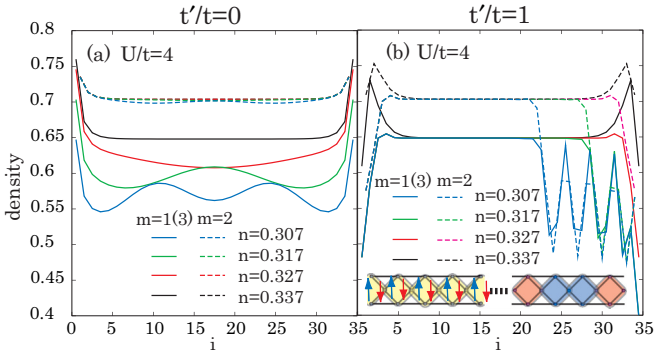

FIG. 5. Density profiles on legs $m = 1,3$ (solid lines) or on $m = 2$ (dashed) for various values of $n \leqslant 1/3$ with $U/t = 4$ for $t' = 0$ (a) or $t'/t = 1$ (b). The system has open boundaries with length $L = 35$ (with $N = 104$ sites in total). The lower band is fully occupied at filling 0.337, which corresponds to 1/3-filling in the periodic boundary. Insets in (b) schematically represent phase separation between plateau region (left inset) and CDW-like (right) region. The plateau is formed by doubly occupied states in the flat-band basis, which corresponds to those in the insulating phase at 1/3-filling, while the CDW-like to a configuration of the localized states with $2\pi/3$-periodicity. Inset of (b) systematically show the CDW-like configuration, where high (red) and low (blue) density regions are aligned with $2\pi/3$-periodicity.

at $m = 1$ or $m = 3$ around the boundary. By contrast, when $t' = -0.2 < 0$, for which we have Fermi points [see Fig. 1(b) in the main text], edge states on $m = 1$ or 3 have a staggered magnetization with an exponential decay off the edge.

Thus we find that the edge states take various structures depending on the value of t'. In all cases, even degeneracies appear only for diagonal cut. This means that the entanglement pair is mainly formed across the legs 1 and 3. Specifically, the edge states for $t'/t = 0$ are sharply localized at the diagonal edge boundary, which suggests that the entanglement pair for $t' = 0$ form dimerlike states across legs 1 and 3.

APPENDIX B: DENSITY PROFILES AND CORRELATIONS BELOW 1/3-FILLING

In order to identify a phase separation (as another pair-binding effect distinct from superfluidity), let us show in Fig. 5 the density profiles calculated with DMRG for open boundary conditions. For $t' = 0$ density profiles below 1/3-filling only show Friedel-like oscillations induced by boundaries. For $t'/t = 1$, by contrast, phase separation between plateau and CDW-like regions is observed. We can analyze this by first noting that particles on the flat band for $t'/t = 1$ can be represented by a basis comprising localized states (see right panel of Fig. 1(c) in the main text),

$$b_{\sigma,i} = c_{2,\sigma,i} + c_{2,\sigma,i+1} - c_{1,\sigma,i+1} - c_{3,\sigma,i+1}\,, \tag{B1}$$

with which we have

$$|\Psi\rangle = \prod_{\sigma,i}(b^{\dagger}_{\sigma,i})^{n_{\sigma,i}}|0\rangle\,, \tag{B2}$$

$$H_{{\rm kin},t'=1}|\Psi\rangle = -2t\sum_{\sigma,i} n_{\sigma,i}|\Psi\rangle\,, \tag{B3}$$

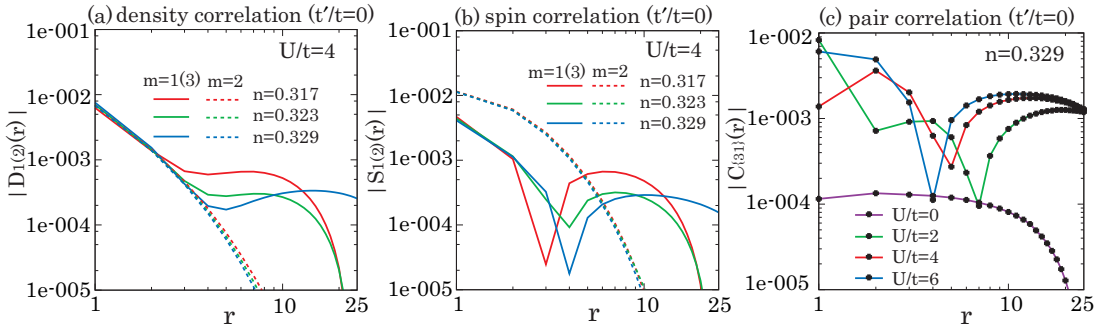

FIG. 6. The absolute value of the density (a) and spin (b) correlation functions on legs $m = 1,3$ (solid lines) or on $m = 2$ (dashed) for various values of $n < 1/3$ with $t'/t = 0$ and $U/t = 4$. (c) is the absolute value of the pair correlation functions $C_{31}(r)$ for various values of U/t with $t'/t = 0$ and $n = 0.329$. All figures are shown on log-log scales. Length of the chain is $L = 55$ with $N = 165$ sites in total and $i_0 = L/4$.

where $n_{\sigma,i}$ is the particle number in the localized state i. The CDW-like region corresponds to a configuration of the localized states $b_{\sigma,i}$ with $2\pi/3$ periodicity, while the plateau region represents doubly occupied states, $b^\dagger_{\downarrow,i}b^\dagger_{\uparrow,i}|0\rangle$, which is the gapped phase formed at 1/3-filling. Although the result for the binding energy (Fig. 2 in the main text) shows a two-particle attraction for $t'/t = 1$, the phase separation observed here implies formation of domains. This contrasts with the case of $t' = 0$, where we have an attractive binding energy but with no phase-separated behavior, which is consistent with formation of itinerant pairs as seen in the pair correlation.

We also display in Fig. 6 the density and spin correlation functions as well as pair correlation, on double-logarithmic scales for various values of n here. As before, correlation functions are calculated for the interior of the finite system. While we have some dip structures due to spatial modulations, the overall decay of the density $D_1(r)$ and spin $S_1(r)$ correlations become slow in the vicinity of 1/3-filling, but not so slowly decaying as the pair correlation. We can again confirm that the behavior is quite sensitive to the values of n and U/t

APPENDIX C: HAMILTONIAN IN THE "WANNIER" BASIS

It is curious how the Hamiltonian, Eq. (1) in the main text, should look like when expressed in "Wannier" basis. For the original diamond chain with $t' = 0$, we can introduce the basis $\alpha_{i,\sigma} = c_{2,i,\sigma}$, $\beta_{i,\sigma} = (c_{1,i,\sigma} + c_{3,i,\sigma})/\sqrt{2}$ for the dispersive bands, and $\gamma_{i,\sigma} = (c_{1,i,\sigma} - c_{3,i,\sigma})/\sqrt{2}$ for the flat band. The interaction term $H_{\rm int}$ can then be expressed as

$$H_{\rm int} = \sum_i h_{{\rm int},i}, \tag{C1}$$

$$h_{{\rm int},i} = \frac{U}{2}\sum_{\lambda,\lambda'=\beta,\gamma} n_{\lambda,\uparrow,i}n_{\lambda',\downarrow,i} + Un_{\alpha,\uparrow,i}n_{\alpha,\downarrow,i} + \frac{U}{2}(\rho^{(+)}_{\beta,i}\rho^{(-)}_{\gamma,i} - S^{(+)}_{\beta,i}S^{(-)}_{\gamma,i} + {\rm H.c.}), \tag{C2}$$

where, for $\lambda = \beta,\gamma$, $n_{\lambda,\sigma,i} = \lambda^\dagger_{\sigma,i}\lambda_{\sigma,i}$, while $S^{(-)}_{\lambda,i} = \lambda^\dagger_{\downarrow,i}\lambda_{\uparrow,i}$ and $S^{(+)}_{\lambda,i} = [S^{(-)}_{\lambda,i}]^\dagger$ are spin-flip operators, and $\rho^{(-)}_{\lambda,i} = \lambda_{\uparrow,i}\lambda_{\downarrow,i}$ and $\rho^{(+)}_{\lambda,i} = [\rho^{(-)}_{\lambda,i}]^\dagger$ pair-hopping operators. The pair-hopping interaction, $\rho^{(+)}_{\beta,i}\rho^{(-)}_{\gamma,i}$, allows a doubly occupied state, $|\Psi\rangle_i = (\beta_{\uparrow,i}\beta_{\downarrow,i} - \gamma_{\uparrow,i}\gamma_{\downarrow,i})^\dagger|0\rangle_i$, to be the lowest eigenstate of an isolated unit cell Hamiltonian, $h_{{\rm int},i}|\Psi\rangle_i = 0$, at 1/3-filling. This is expected to favor pair formation. Indeed, $\beta_{\uparrow,i}\beta_{\downarrow,i} - \gamma_{\uparrow,i}\gamma_{\downarrow,i}$ is nothing but the singlet pair in the original bases, $\Delta_{31,i} = c_{3,i,\uparrow}c_{1,i,\downarrow} - c_{3,i,\downarrow}c_{1,i,\uparrow}$ considered in the main text.

APPENDIX D: BINDING ENERGY FOR VARIOUS VALUES OF U/t

Figure 7 plots the binding energy against the density n and t'/t for various values of U/t. Attractive binding energies are found also above 1/3-filling at $U/t = 6$, but development of pair correlation is not found in ED and DMRG calculations for the sample sizes treated here.

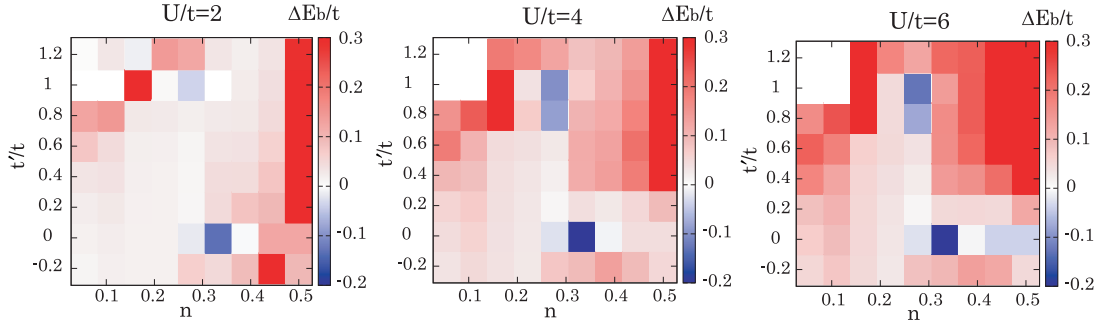

FIG. 7. Color-code plot of $\Delta E_{\rm b}$ against n and t'/t for various values of U/t.

[1] E. H. Lieb, Phys. Rev. Lett. **62**, 1201 (1989); **62**, 1927 (1989).

[2] A. Mielke, J. Phys. A: Math. Gen. **24**, L73 (1991); **24**, 3311 (1991).

[3] H. Tasaki, Phys. Rev. Lett. **69**, 1608 (1992).

[4] H. Tasaki, Prog. Theor. Phys. **99**, 489 (1998).

[5] See, e.g., references in M. G. Yamada, T. Soejima, N. Tsuji, D. Hirai, M. Dincă, and H. Aoki, Phys. Rev. B **94**, 081102(R) (2016), which proposes a design of a flat-band ferromagnetism in an organometallic system.

[6] S. Taie, H. Ozawa, T. Ichinose, T. Nishio, S. Nakajima, and Y. Takahashi, Sci. Adv. **1**, e1500854 (2015).

[7] G.-B. Jo, J. Guzman, C. K. Thomas, P. Hosur, A. Vishwanath, and D. M. Stamper-Kurn, Phys. Rev. Lett. **108**, 045305 (2012).

[8] E. Tang, J.-W. Mei, and X.-G. Wen, Phys. Rev. Lett. **106**, 236802 (2011).

[9] K. Sun, Z. Gu, H. Katsura, and S. Das Sarma, Phys. Rev. Lett. **106**, 236803 (2011).

[10] T. Neupert, L. Santos, C. Chamon, and C. Mudry, Phys. Rev. Lett. **106**, 236804 (2011).

[11] X. Li, E. Zhao, and W. V. Liu, Nat. Commun. **4**, 1523 (2013).

[12] M. Tovmasyan, S. Peotta, P. Törmä, and S. D. Huber, arXiv:1608.00976, study the attractive Hubbard model to discuss the superfluid weight of a flat band.

[13] R. R. Montenegro-Filho and M. D. Coutinho-Filho, Phys. Rev. B **74**, 125117 (2006).

[14] J. Vidal, B. Douçot, R. Mosseri, and P. Butaud, Phys. Rev. Lett. **85**, 3906 (2000); B. Douçot and J. Vidal, *ibid.* **88**, 227005 (2002).

[15] K. Kuroki, T. Higashida, and R. Arita, Phys. Rev. B **72**, 212509 (2005).

[16] S. Takayoshi, H. Katsura, N. Watanabe, and H. Aoki, Phys. Rev. A **88**, 063613 (2013).

[17] M. Tovmasyan, E. P. L. van Nieuwenburg, and S. D. Huber, Phys. Rev. B **88**, 220510(R) (2013).

[18] S. R. White, Phys. Rev. Lett. **69**, 2863 (1992); Phys. Rev. B **48**, 10345 (1993).

[19] K. A. Hallberg, Adv. Phys. **55**, 477 (2006); U. Schollwöck, Ann. Phys. (NY) **326**, 96 (2011).

[20] M. Okumura, S. Yamada, M. Machida, and T. Sakai, Phys. Rev. A **79**, 061602(R) (2009).

[21] M. Okumura, S. Yamada, M. Machida, and H. Aoki, Phys. Rev. A **83**, 031606(R) (2011).

[22] To minimize the effect of edges, we calculate correlation functions for an interior region as [23] $C(r) = \frac{1}{L-2i_0-r}\sum_{i_0<i}^{L-i_0-r} C(i+r,i)$, where $C(i+r,i)$ stands for the two-point correlation function and i_0 ($=L/4$ in Fig. 3) is set well away from the sample edges.

[23] A. M. Lobos, M. Tezuka, and A. M. Garcia-Garcia, Phys. Rev. B **88**, 134506 (2013).

[24] The magnitude of the pair correlation $\sim 10^{-3}$ is similar to those numerically calculated for the standard ladder systems such as the three-leg Hubbard ladder; see, e.g., T. Kimura, K. Kuroki, and H. Aoki, Phys. Rev. B **54**, R9608 (1996); J. Phys. Soc. Jpn. **66**, 1599 (1997); **67**, 1377 (1998).

[25] Z. Gulacsi, A. Kampf, and D. Vollhardt, Phys. Rev. Lett. **99**, 026404 (2007).

[26] H. Kikuchi, Y. Fujii, M. Chiba, S. Mitsudo, T. Idehara, T. Tonegawa, K. Okamoto, T. Sakai, T. Kuwai, and H. Ohta, Phys. Rev. Lett. **94**, 227201 (2005).

[27] H. Jeschke, I. Opahle, H. Kandpal, R. Valenti, H. Das, T. Saha-Dasgupta, O. Janson, H. Rosner, A. Brühl, B. Wolf, M. Lang, J. Richter, S. Hu, X. Wang, R. Peters, T. Pruschke, and A. Honecker, Phys. Rev. Lett. **106**, 217201 (2011).

[28] G. Vidal, J. I. Latorre, E. Rico, and A. Kitaev, Phys. Rev. Lett. **90**, 227902 (2003).

[29] V. E. Korepin, Phys. Rev. Lett. **92**, 096402 (2004).

[30] F. Pollmann, A. M. Turner, E. Berg, and M. Oshikawa, Phys. Rev. B **81**, 064439 (2010).

[31] F. Pollmann, E. Berg, A. M. Turner, and M. Oshikawa, Phys. Rev. B **85**, 075125 (2012).

[32] I. Affleck, T. Kennedy, E. H. Lieb, and H. Tasaki, Phys. Rev. Lett. **59**, 799 (1987); Commun. Math. Phys. **115**, 477 (1988).

[33] K. Hida, J. Phys. Soc. Jpn. **85**, 024705 (2016).

[34] M. Arikawa, S. Tanaya, I. Maruyama, and Y. Hatsugai, Phys. Rev. B **79**, 205107 (2009).